



**HAL**  
open science

# A Parametric Study of Additive Manufacturing Process: TA6V Laser Wire Metal Deposition

Valentine Cazaubon, Audrey Abi Akle, Xavier Fischer

## ► To cite this version:

Valentine Cazaubon, Audrey Abi Akle, Xavier Fischer. A Parametric Study of Additive Manufacturing Process: TA6V Laser Wire Metal Deposition. Lecture Notes in Mechanical Engineering, 2021, Advances on Mechanics, Design Engineering and Manufacturing III Proceedings of the International Joint Conference on Mechanics, Design Engineering & Advanced Manufacturing, JCM 2020, June 2-4, 2020, pp.15 - 20. 10.1007/978-3-030-70566-4\_4 . hal-03299893

**HAL Id: hal-03299893**

**<https://hal.science/hal-03299893>**

Submitted on 26 Jul 2021

**HAL** is a multi-disciplinary open access archive for the deposit and dissemination of scientific research documents, whether they are published or not. The documents may come from teaching and research institutions in France or abroad, or from public or private research centers.

L'archive ouverte pluridisciplinaire **HAL**, est destinée au dépôt et à la diffusion de documents scientifiques de niveau recherche, publiés ou non, émanant des établissements d'enseignement et de recherche français ou étrangers, des laboratoires publics ou privés.



# A Parametric Study of Additive Manufacturing Process: TA6V Laser Wire Metal Deposition

Valentine Cazaubon<sup>1,2</sup>(✉), Audrey Abi Akle<sup>1</sup>, and Xavier Fischer<sup>1,2</sup>

<sup>1</sup> Univ. Bordeaux, ESTIA Institute of Technology, 64210 Bidart, France  
v.cazaubon@estia.fr

<sup>2</sup> Arts et Metiers Institute of Technology, University of Bordeaux, CNRS, Bordeaux INP, INRAE, I2M Bordeaux, 33400 Talence, France

**Abstract.** Additive Manufacturing has proven to be an economically and industrially attractive process in building or repairing parts. However, the major issue of this new process is to guarantee a mechanical behavior identical to the subtractive manufacturing methodologies. The work, presented in this paper, is centered on the Laser Wire Metal Deposition (LMD-w) method with the metallic alloy TA6V. Its working principle is to fuse a coaxial wire on a substrate with a laser as a heat source. To better understand the interaction between the input parameters (Laser Power, Wire Feed Speed and Tool Speed) and the clad geometry output variables (Height, Width and Contact Angle) and the substrate displacement, we have realized an experimentation. We printed 9 clads according Taguchi's experimental design. Pearson correlation coefficient and Fisher test performed on the experimental measures showed as main result: Tool Speed is the parameter with the most significant influence on the output variables.

**Keywords:** Parameters influences · Clads geometry · Clads characterization · Taguchi's experimental design · Statistical analysis

## 1 Introduction

American Society for Testing Material (ASTM) has defined additive manufacturing (AM) as “a process of joining materials to make objects from 3D model data, usually layer upon layer, as opposed to subtractive manufacturing methodologies” [1]. AM has proven to be an economically and industrially attractive process. It achieves a buy-to-fly ratio, weight ratio between the raw material used for a part and the weight of the part, of 1:1 [2]. The wire processes allow to obtain a 99,6% deposit yield [3]. From the 7 categories of additive manufacturing processes [4] our work focuses on the Laser Wire Metal Deposition (LMD-w). Moreover, three alloys of materials are used in AM: Inconel, 316L steel and TA6V. Among them, the titanium alloy (TA6V) has low resistance to oxidation but presents the advantages of low density and high resistance to corrosion [5, 6]; that is why we have chosen to work with TA6V wire.

One major issue of AM process is to guarantee a mechanical behavior identical to the subtractive manufacturing methodologies. In this paper, we present our study

about the influences of first order input parameters on the geometric aspects and on the displacement of the substrate, metal part on which the molten wire is deposited to print the geometry [7]. To do so, we have performed an experimental campaign and have analyzed resulting data. The analysis consisted of two stages: the analysis of the correlation with the Pearson coefficient and an analysis of the variance with the Fisher test.

## 2 Protocol of Experiments

### 2.1 Model and Variables

Following the LMD-w process, the TA6V wire is deposited on the substrate, into the melting pool with a speed WFS coaxially to the laser at a power P while the robotic head is moving at a speed TS, Fig. 1.

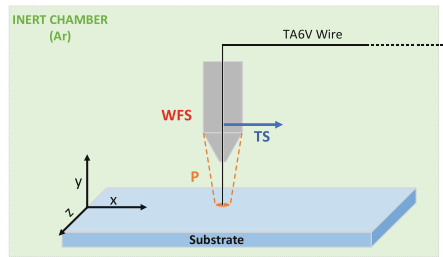


**Fig. 1.** Schematic representation of the LMD-w process input parameters

**Table 1.** LMD-W input parameters and measured outputs studied

Nature	Name	Representation	Units	Domain
Input parameters	Laser power	P	W	[1680; 2000]
	Wire feed speed	WFS	m/min	[1,5; 2,1]
	Tool speed	TS	m/min	[0,2; 0,8]
Outputs	Clad height	$h_c$	mm	Measured
	Dilution height	$h_d$	mm	
	Clad width	$w_c$	mm	
	Dilution width	$w_d$	mm	
	Contact angle	$\alpha$	°	
	Substrate displacement	d	mm	

The LMD-w process is modeled with input and output variables presented in Table 1. The objective of the experiments is to define relations between the outputs and the inputs in order to predict the clad's geometry according to a parameter combination.

## 2.2 Methods

We used, as substrates, plates of TA6V of dimensions  $150 \text{ mm} \times 60 \text{ mm} \times 5 \text{ mm}$  which have been sanded with orbital grinder (grain P60) and degreased with isopropyl alcohol (IPA). This surface treatment helps to improve surface laser absorptivity and to remove dusts. The deposit wire material is TA6V of 1.2 mm. The substrate and wire are made of titanium because of its weldability properties [8]. The substrate is bridled preventing any translational movements in the plan  $(x, y)$ . TA6V is supplied by Technalloy. To protect the melting pool from oxidation, we have built the clads in an inert chamber with a protective gas: argon as recommended [6].

The inert chamber is part of a robotized cell. The cell is composed of a 6-axis robot (KUKA KR60-HA) with its controller (KUKA KRC4). The energy is bringing by a laser head (PRECITEC CoaxPrinter) fixed on the robot. As described in Fig. 1, the wire deposition is coaxial to the laser.

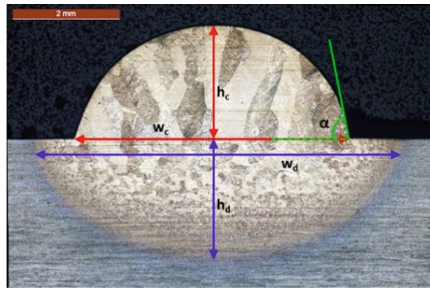


**Fig. 2.** Cross section micrograph of TA6V deposit ( $\times 5$ ). Outputs: red: clad height, green: dilution height, blue: clad width and white: dilution width.

Nine clads of 100 mm length have been deposited on each substrate. Three cuts have been made on each substrate (i.e.  $\frac{1}{4}$  cord length,  $\frac{1}{2}$  cord length and  $\frac{3}{4}$  cord length) using a silicon disc and a cutting wheel. Subsequently, the samples are coated, mirror polished and then chemically attacked with Kroll's reagent. The measurements will be carried out under a microscope (LEICA DM1750 M) and its software Leica Application Suite (see example in Fig. 2).

## 2.3 Taguchi's Experimental Design

We know according to [7] the interactions between the input parameters can be neglected. The model is a linear expression of the outputs based on the input parameters. The coefficients of the model can be calculated only after performing the experiments. In absence of these coefficients, we write the model symbolically in order to clarify the parameters inputs considered. Thus, we obtained the studied model described by the Eq. (1), with  $y$  an output and  $M$  the average of the output's values as the constant term. As we would like to know if there are (non-)linearity between the input and the output variables, we defined three levels for the input parameters P, WFS and TS. To determine

the number of experiments, we used Taguchi’s experimental design based on the use of orthogonal tables.

$$y = M + P + WFS + TS \tag{1}$$

Following the Taguchi rules, we must know the total degree of freedom (tfd) of our model (Eq. (1)) and the Least Common Multiple (LCM). With our model, we obtained tfd equals 8 and LCM equals 9. So, the chosen table contains 9 experiments ( $L_9(3^3)$ ). The Table 2 gathers the input parameters and measured outputs.

**Table 2.** Inputs parameters and measured responses

N	Input parameters			Outputs					
	<i>P</i> (W)	<i>WFS</i> (m/min)	<i>TS</i> (m/min)	<i>d</i> (mm)	<i>h<sub>c</sub></i> (mm)	<i>h<sub>d</sub></i> (mm)	<i>w<sub>c</sub></i> (mm)	<i>w<sub>d</sub></i> (mm)	<i>α</i> (°)
1	1680	1.5	0.2	1.978	2.148	2.2033	5.151	6.939	75
2	1680	1.8	0.4	0.892	1.742	1.2847	3.832	4.873	76
3	1680	2.1	0.6	1.357	1.533	0.9797	3.493	4.067	87
4	1840	1.5	0.4	1.235	1.353	1.5443	4.480	5.633	55
5	1840	1.8	0.6	1.125	1.213	1.1723	3.878	4.826	56
6	1840	2.1	0.2	1.910	3.038	2.0567	4.306	6.320	103
7	2000	1.5	0.6	0.443	0.960	1.2713	4.345	5.232	39
8	2000	1.8	0.2	1.635	2.361	2.6157	5.726	7.592	72
9	2000	2.1	0.4	1.177	1.783	1.4057	4.493	5.571	71

### 3 Results and Analysis

#### 3.1 Correlation Coefficient

The correlation coefficient was calculated using the Pearson’s method with R software. We used it to determine whether the relationship between an input parameter and a measured output is linear or not and if it is positive or negative. If  $|r| > 0.6$ , the two studied variables tend to have a linear relationship [9]. Table 3 presents the correlation coefficients and their significance.

**Table 3.** Pearson’s coefficient between the input parameters and the outputs with their significance

Input parameters	Outputs					
	<i>h<sub>c</sub></i>	<i>h<sub>d</sub></i>	<i>w<sub>c</sub></i>	<i>w<sub>d</sub></i>	<i>d</i>	<i>α</i>
P	-0.05	0.21	0.42*	0.32	-0.27	0.40*
WFS	0.45*	-0.11	-0.31	-0.20	0.26	0.69***
TS	-0.86***	-0.91***	-0.73***	-0.87***	-0.77***	-0.50**

P-value (0; 0.001; 0.01; 0.05; 0.1) – Respective Symbols (:\*\*\*; \*\*, \*;).

The analysis establishes WFS and  $\alpha$  follow a positive linear law with  $r = 0.69$  and  $p\text{-value} < 0.001$ . The results allow to conclude to negative linear relationships between TS and bead's geometries ( $h_c$  and  $w_c$ ), TS and dilution's geometries ( $h_d$  and  $w_d$ ) and TS and the substrate's displacement ( $d$ ).

### 3.2 Variance Analysis

The Fisher-Snedecor test compares the variance. It has been performed between each input parameters' levels and output variables. The null hypothesis saying the variables are not independent would be rejected if the F value calculated (F) is superior to the F value read in the Snedecor table ( $F_{SNEDECOR}$ ).  $F > F_{SNEDECOR}(2, 3)$  with a  $p\text{-value} < 0,05$ . The Table 4 gathers the results of Fisher-Snedecor Test coefficients. If the value of  $F(2, 3)$  is above 9.55 then the  $p\text{-value} < 0,05$  and we can reject statistical hypothesis  $H_0$ . Thus, for the model (1) the results allow concluding TS is the only input parameter to exert a significant influence on all the responses observed. However,  $h_c$  also depends significantly on the WFS input parameter. Only the contact angle  $\alpha$  is significantly dependent on the three input parameters.

**Table 4.** Fisher test results and their p-values

Input		$h_c$	$h_d$	$w_c$	$w_d$	$\alpha$	$d$
P	F	0.94	3.60	4.63	9.25	15.63	1.45
	p-value	0.4811	0.1594	0.1210	0.0521	0.0259	0.3617
WFS	F	13.27	2.53	2.57	5.17	42.14	0.92
	p-value	0.0324	0.2269	0.2236	0.1068	0.0064	0.4882
TS	F	57.21	67.48	10.93	68.14	23.50	8.70
	p-value	0.0041	0.0032	0.0419	0.0032	0.0147	0.0564

## 4 Conclusion

The study carried out on the LMD-W process analyses the influence of the input parameters (Power, Wire Feed Speed and Tool Speed) on the clad geometry output variables. According to Taguchi's experimental design, 9 clads were printed. The correlation coefficients and the Fisher test allow to conclude Tool Speed is the parameter with the most significant influence on the clads geometry. Five out of six measured output variables follow a linear law with Tool Speed. The clad height is also dependent on the Wire Feed Speed parameter. However, the contact angle is the only response to dependent on the three input parameters. It is therefore possible to model all these responses according to a multiple linear regression using the Least Squares method .

**Acknowledgments.** The research work reported here was made possible by the Fonds Unique Interministériel (FUI Addimafil).

## References

1. Frazier, W.E.: Metal additive manufacturing: a review. *J. Mater. Eng. Perform.* **23**(6), 1917–1928 (2014)
2. Lundbäck, A., Lindgren, L.E.: Finite element simulation to support sustainable production by additive manufacturing. *Procedia Manuf.* **7**, 127–130 (2017)
3. Javidani, M., Arreguin-Zavala, J., Danovitch, J., Tian, Y., Brochu, M.: Additive manufacturing of AlSi10Mg alloy using direct energy deposition: microstructure and hardness characterization. *J. Therm. Spray Technol.* **26**(4), 587–597 (2017)
4. Price, A.: Additive Manufacturing – Standards (2013). <https://www.nottingham.ac.uk/research/groups/advanced-manufacturing-technology-research-group/documents/manufacturing-metrology-team/qcam-17/bsi.pdf>. Accessed 6 Feb 2020
5. Peters, M., Kumpfert, J., Ward, C.H., Leyens, C.: Titanium alloys for aerospace application. *Adv. Eng. Mater.* **5**(6), 419–427 (2003)
6. Zwilling, V., Darque-Ceretti, E., Boutry-Forveille, A., David, D., Perrin, M.Y., Aucouturier, M.: Structure and physicochemistry of anodic oxide films on titanium and TA6V alloy. *Surf. Interface Anal.* **27**(7), 629–637 (1999)
7. Medrano Téllez, A.G.: Fibre laser metal deposition with wire: parameters study and temperature control. Doctoral dissertation, University of Nottingham (2010)
8. Ranatowski, E.: Weldability of titanium and its alloys-progress in joining. *Adv. Mater. Sci.* **8**(2), 69–76 (2008)
9. Benesty, J., Chen, J., Huang, Y., Cohen, I.: Pearson correlation coefficient. In: *Noise Reduction in Speech Processing*, pp. 1–4. Springer, Heidelberg (2009)

**Open Access** This chapter is licensed under the terms of the Creative Commons Attribution 4.0 International License (<http://creativecommons.org/licenses/by/4.0/>), which permits use, sharing, adaptation, distribution and reproduction in any medium or format, as long as you give appropriate credit to the original author(s) and the source, provide a link to the Creative Commons license and indicate if changes were made.

The images or other third party material in this chapter are included in the chapter's Creative Commons license, unless indicated otherwise in a credit line to the material. If material is not included in the chapter's Creative Commons license and your intended use is not permitted by statutory regulation or exceeds the permitted use, you will need to obtain permission directly from the copyright holder.

